FORMULATION AND EVALUATION OF CIMETIDINE LOADED BILOSOMES FOR ENHANCED DRUG DELIVERY

[1]Sundhararajan R, [2]Rajalakshmi G, [3]Sowmiya K*
[1]Principal, Department of Pharmaceutical Chemistry, Mohamed Sathak A.J. College of Pharmacy
[2]Associate Professor, Department of Pharmaceutics, Mohamed Sathak A.J. College of Pharmacy
[3]Department of Pharmaceutics, Mohamed Sathak A.J. College of Pharmacy
The Tamilnadu DR.M.G.R Medical University, India
Corresponding Author: Sowmiya K

Received: Aug 15, 2026 Accepted: Sep 12, 2026 Published: Sep 15, 2026

Abstract

The present study aimed to develop and evaluate cimetidine-loaded bilosomes as a lipid-based vesicular system for sustained oral drug delivery. Cimetidine-loaded bilosomes were prepared using sodium deoxycholate (SDC), soy phosphatidylcholine (SPC), cholesterol, and Span 60 as principal vesicle-forming components. Nine formulations (F1–F9) were developed by varying the concentrations of the lipid and surfactant components while maintaining cimetidine at 200 mg. The aqueous solubility of cimetidine was found to be 10.25 ± 0.08 mg/mL. UV-visible spectrophotometric analysis established a λmax of 229 nm, and the calibration curve showed excellent linearity over 2–20 µg/mL, with a regression equation of y = 0.0442x + 0.0175 and R^2 = 0.9968. Entrapment efficiency varied from 67.60 ± 1.21% to 84.70 ± 0.72%, with F6 exhibiting the highest entrapment efficiency. The optimized F6 formulation contained 0.3 g SDC, 0.3 g SPC, 0.8 g cholesterol, and 0.2 g Span 60. Particle-size analysis demonstrated a nanosized vesicular population of approximately 150 nm with a PDI of 0.222 ± 0.004. The zeta potential of approximately −50 mV indicated favorable colloidal stability. SEM revealed predominantly spherical to near-spherical vesicles, while FTIR analysis supported compatibility between cimetidine and the formulation components. All formulations exhibited prolonged drug release over 24 h. F6 demonstrated a controlled release profile, achieving 90.36 ± 1.39% cumulative drug release at 24 h. Overall, F6 showed promising entrapment, nanoscale characteristics, stability, and sustained drug release, supporting further investigation of cimetidine-loaded bilosomes as a potential oral lipid-based delivery system.

Keywords: Cimetidine; Bilosomes; Sodium deoxycholate; Nanovesicles; Sustained drug delivery.

INTRODUCTION

1.1.Overview of Oral Drug Delivery

Oral administration is one of the most widely employed approaches for the delivery of therapeutic agents because of its convenience, simplicity, patient acceptability, and suitability for both acute and chronic pharmacotherapy. Compared with invasive routes of administration, oral drug delivery generally provides greater patient comfort, reduces the requirement for trained healthcare personnel, and facilitates self-administration. These characteristics have made oral dosage forms such as tablets, capsules, solutions, suspensions, and multiparticulate systems important components of modern pharmaceutical therapy.

Despite its widespread acceptance, successful oral drug delivery depends on a complex sequence of physicochemical and physiological events. Following administration, a drug must be released from its dosage form, dissolve in gastrointestinal fluids, remain sufficiently stable within the gastrointestinal tract, reach an appropriate site of absorption, cross the intestinal epithelial barrier, and subsequently enter the systemic circulation. Failure at any one of these stages can substantially reduce the fraction of the administered dose reaching systemic circulation [1].

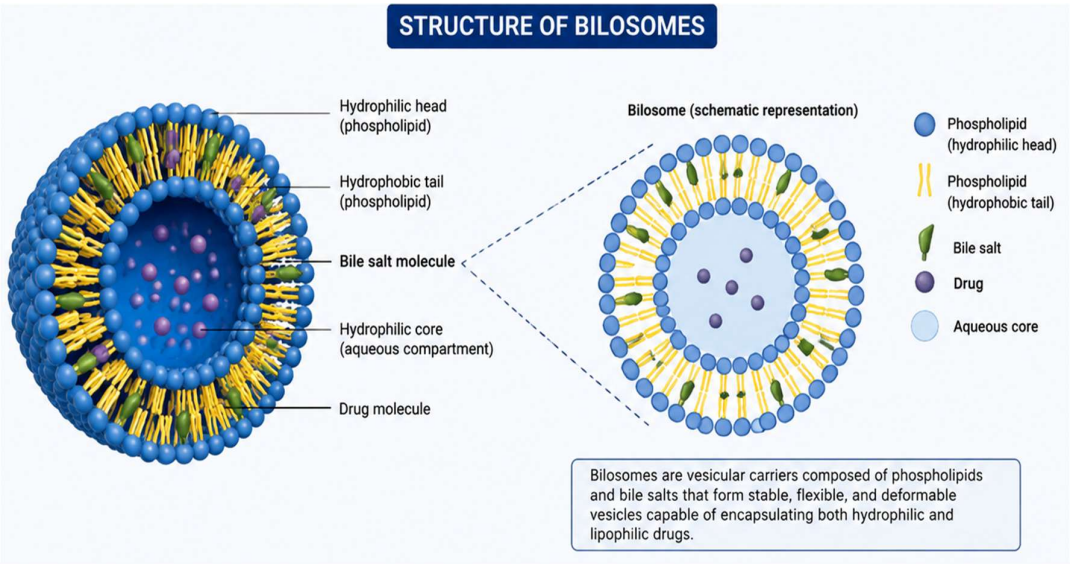

Figure 1: Structure of bilosomes

Aim

To formulate and evaluate cimetidine-loaded bilosomal nanocarriers for improving oral drug delivery, enhancing entrapment efficiency, and achieving sustained drug release.

Objectives

1. To evaluate the compatibility of cimetidine with selected excipients using Fourier Transform Infrared Spectroscopy (FTIR).
2. To prepare cimetidine-loaded bilosomes using the thin-film hydration technique with varying concentrations of sodium deoxycholate, soy phosphatidylcholine, cholesterol, and Span 60.
3. To characterize the prepared bilosomal formulations for particle size, polydispersity index (PDI), and zeta potential.
4. To study the surface morphology of the optimized bilosomal formulation using Scanning Electron Microscopy (SEM).
5. To determine the entrapment efficiency of cimetidine-loaded bilosomal formulations.
6. To evaluate the *in vitro* drug release profile of cimetidine-loaded bilosomes.
7. To perform stability studies of the optimized formulation under different storage conditions.

SCOPE OF THE STUDY

The present study focuses on the formulation and evaluation of cimetidine-loaded bilosomal nanocarriers intended to improve oral drug delivery and enhance therapeutic performance of Cimetidine. The work aims to develop a stable bilosomal system capable of improving drug entrapment, protecting the drug from degradation in the gastrointestinal environment, and providing sustained drug release for prolonged therapeutic action. The study includes the preparation of bilosomes using the thin-film hydration method with suitable concentrations of sodium deoxycholate, soy phosphatidylcholine, cholesterol, and Span 60 to optimize vesicular characteristics.

The scope of the work also includes pre-formulation studies to evaluate the compatibility between cimetidine and selected excipients using FTIR analysis. The prepared formulations will be systematically characterized for particle size, polydispersity index, and zeta potential

to determine vesicle stability and uniformity. Entrapment efficiency studies will be carried out to assess the drug-loading capacity of the bilosomal formulations. Surface morphology of the optimized formulation will be examined using scanning electron microscopy to study vesicle shape and surface characteristics. In addition, *in vitro* drug release studies will be conducted to evaluate the sustained-release behavior of the bilosomal system. Stability studies of the optimized formulation will also be performed under different storage conditions according to ICH guidelines to determine formulation stability, integrity, and shelf life.

1.1.Drug profile

Cimetidine

Category: Histamine H2-receptor antagonist

Chemical Name: N″-cyano-N-methyl-N′-[2-[[(5-methyl-1H-imidazol-4-yl)methyl]thio]ethyl]guanidine

Molecular Formula: $C_{10}H_{16}N_6S$

Molecular Weight: 252.34 g/mol

Description:
Cimetidine is a white to off-white crystalline powder with a characteristic sulfur-like odor. It is widely used in the treatment of gastric ulcers, duodenal ulcers, gastroesophageal reflux disease (GERD), and other acid-related gastrointestinal disorders.

BCS Classification: BCS Class III drug (high solubility and low permeability)

Solubility:
Moderately soluble in water and compatible with lipid-based excipients used in vesicular drug delivery systems.

Mechanism of Action:
Cimetidine competitively inhibits histamine at H2 receptors present on gastric parietal cells, thereby reducing gastric acid secretion and decreasing both basal and stimulated acid output.

Pharmacokinetics:

Bioavailability: Approximately 60–70%

Half-life: 2 hours

Protein Binding: 15–20%

Metabolism: Hepatic metabolism

Excretion: Primarily through urine

Rationale for Selection:

Cimetidine exhibits low membrane permeability, which may reduce its absorption and therapeutic efficiency. Formulation into bilosomal vesicles may improve permeability, sustain drug release, enhance gastrointestinal residence time, and improve oral bioavailability.

1.1.Solubility Studies

The solubility of cimetidine in aqueous medium was determined using the flask-shake method. Excess quantities of pure cimetidine were separately added to glass stoppered tubes containing 10 mL of distilled water. The tubes were placed in an orbital shaker and maintained at 37 ± 1 °C for 36 hours to attain equilibrium. After completion of the shaking period, the samples were filtered through a membrane filter to remove undissolved drug particles. The filtrates were suitably diluted and analyzed using a UV–visible spectrophotometer at the predetermined λmax of cimetidine (229 nm). The obtained absorbance values were used to calculate the solubility of the drug [57].

1.2.Fourier Transform Infrared Spectroscopy (FTIR)

FTIR spectroscopy was carried out to evaluate the compatibility between cimetidine and the excipients used in the bilosomal formulation. The FTIR spectra of pure cimetidine and the cimetidine-loaded bilosomal formulation were recorded using an FTIR spectrophotometer. The samples were placed directly in the sample holder, and spectra were scanned over the wavelength range of 4000–400 cm^{-1} at a resolution of 4 cm^{-1}. The characteristic peaks of cimetidine were identified and compared with those of the formulation to determine any possible chemical interaction or structural modification.

1.3.Preparation of Cimetidine-Loaded Bilosomes

Cimetidine-loaded bilosomes were prepared by the thin-film hydration method. Accurately weighed quantities of cimetidine, cholesterol, Span 60, and soybean phosphatidylcholine were dissolved in a chloroform:methanol mixture (1:1 v/v) in a round-bottom flask. The organic solvents were evaporated under reduced pressure using a rotary vacuum evaporator until a thin and uniform lipid film was formed on the inner wall of the flask. The dried lipid film was hydrated using phosphate-buffered saline (PBS, pH 7.4) containing sodium deoxycholate under continuous stirring to obtain bilosomal vesicles. The resulting dispersion was sonicated for three cycles of 3 minutes each with intermittent cooling periods of 5 minutes to reduce vesicle size and obtain nanosized bilosomes. The prepared cimetidine-loaded bilosomal formulations were collected and stored in airtight glass containers at 4 °C until further evaluation [59].

Table 1: Formulation of cimetidine loaded bilosomes

Formulation	Cimetidine (mg)	SDC (g)	SPC (g)	Cholesterol (g)	Span 60 (g)	Chloroform (mL)
F1	200	0.1	0.1	0.2	0.2	10
F2	200	0.1	0.2	0.4	0.4	10
F3	200	0.1	0.3	0.8	0.8	10
F4	200	0.3	0.1	0.2	0.4	10
F5	200	0.3	0.2	0.4	0.8	10
F6	200	0.3	0.3	0.8	0.2	10
F7	200	0.5	0.1	0.4	0.2	10
F8	200	0.5	0.2	0.8	0.4	10
F9	200	0.5	0.3	0.2	0.8	10

1.4.Evaluation of Particle Size, Polydispersity Index, and Zeta Potential

The average vesicle size, polydispersity index (PDI), and zeta potential of the prepared cimetidine-loaded bilosomes were determined using a Malvern Zetasizer. The formulations were diluted appropriately with distilled water prior to analysis to avoid multiple scattering effects. Particle size and PDI were measured by dynamic light scattering technique using

disposable cuvettes. Zeta potential was determined using a zeta potential cell equipped with electrodes. All measurements were performed in triplicate at room temperature.

1.5.Determination of Entrapment Efficiency

The entrapment efficiency of cimetidine-loaded bilosomes was determined by centrifugation method. Approximately 0.5 mL of bilosomal dispersion was mixed with phosphate-buffered saline and centrifuged at 13,000 rpm for 60 minutes at 4 °C. The supernatant containing free drug was separated carefully, and the amount of unentrapped cimetidine was analyzed spectrophotometrically at the selected wavelength.

The percentage entrapment efficiency (EE%) was calculated using the following equation:

$$EE\ (\%) = [(\text{Total drug} - \text{Free drug}) / \text{Total drug}] \times 100$$

where,

- Total drug represents the amount of cimetidine initially added during formulation.
- Free drug represents the amount of unentrapped cimetidine present in the supernatant [61].

1.6.Scanning Electron Microscopy (SEM)

The surface morphology of the optimized cimetidine-loaded bilosomal formulation was examined using scanning electron microscopy (SEM). A small quantity of the dried formulation was mounted on a metal stub using double-sided adhesive tape and coated with a thin layer of gold under vacuum to render the sample electrically conductive. The coated samples were observed under the SEM at suitable magnifications, and micrographs were recorded to evaluate the shape, surface characteristics, and distribution of the bilosomal vesicles [60].

1.7.Estimation of drug content

The drug content of Cimetidine-loaded bilosomes was determined by UV–Visible spectrophotometric analysis. An accurately measured quantity of bilosomal dispersion equivalent to the required amount of cimetidine was transferred into a volumetric flask and treated with methanol to rupture the vesicles and extract the entrapped drug completely. The

mixture was sonicated for 10–15 minutes and the volume was adjusted with methanol or phosphate buffer. The resulting solution was centrifuged at 10,000 rpm for 15 minutes to remove lipidic debris and other insoluble materials. The clear supernatant was suitably diluted and analyzed using a UV–Visible spectrophotometer at 229 nm against a suitable blank. The amount of drug present was calculated using the calibration curve of cimetidine. The analysis was carried out in triplicate, and the results were expressed as mean ± standard deviation [40].

1.8.In vitro Drug Release Studies

The *in vitro* drug release study of cimetidine-loaded bilosomes was carried out using an open-ended diffusion tube method. A pre-soaked cellophane membrane was securely tied to one end of the diffusion tube, which served as the donor compartment. The receptor compartment contained 200 mL of phosphate buffer solution (pH 7.4) maintained at 37 ± 2 °C under continuous stirring using a magnetic stirrer. An accurately measured quantity of bilosomal formulation was placed in the donor compartment. At predetermined time intervals, aliquots of the receptor medium were withdrawn and replaced immediately with an equal volume of fresh phosphate buffer to maintain sink conditions. The withdrawn samples were analyzed using a UV–visible spectrophotometer at the λmax of cimetidine (229 nm), and the cumulative percentage drug release was calculated.

1.9.Stability Studies

Stability studies of the optimized cimetidine-loaded bilosomal formulation were performed under two different storage conditions: room temperature (25 ± 2 °C) and refrigerated condition (4 ± 2 °C). The formulations were stored in tightly closed glass vials for a period of 30 days. Samples were withdrawn at predetermined intervals (0 & 30 day) and evaluated for physical appearance, vesicle size, polydispersity index, zeta potential, entrapment efficiency, and drug content. The obtained results were compared with the initial values to determine the physical and chemical stability of the prepared bilosomal formulations during storage.

RESULTS AND DISCUSSION

1.10. Solubility studies

The aqueous solubility of cimetidine was determined by the flask-shake method at 37 ± 1 °C after an equilibration period of 36 h. The samples were analyzed spectrophotometrically at the

predetermined maximum wavelength (λmax = 229 nm). The equilibrium solubility values obtained from three replicate determinations were 10.18, 10.33, and 10.25 mg/mL, respectively, giving a mean aqueous solubility of 10.25 ± 0.08 mg/mL.

The relatively small standard deviation observed among the replicate measurements indicated good reproducibility of the solubility determination. The results suggest that cimetidine possesses appreciable aqueous solubility under the experimental conditions. This characteristic is advantageous for dissolution of the drug in gastrointestinal fluids; however, aqueous solubility alone does not necessarily ensure efficient oral absorption because membrane permeability can also influence the extent of drug absorption.

The observed solubility characteristics are particularly relevant to the development of cimetidine-loaded bilosomes. As cimetidine is relatively hydrophilic, a substantial proportion of the drug may preferentially associate with the aqueous compartment of the bilosomal dispersion rather than the hydrophobic region of the vesicular bilayer. Consequently, formulation variables such as SPC, cholesterol, Span 60, and sodium deoxycholate concentrations should be optimized to achieve adequate drug entrapment while minimizing leakage of the drug from the vesicles.

Overall, the equilibrium aqueous solubility of cimetidine was found to be 10.25 ± 0.08 mg/mL, demonstrating satisfactory solubilization in aqueous medium. These findings provide useful preliminary information for subsequent formulation development and optimization of cimetidine-loaded bilosomes.

1.11. Construction of calibration curve

The calibration curve of cimetidine was developed using a series of standard solutions ranging from 2 to 20 µg/mL. The absorbance of each standard solution was measured using a UV–visible spectrophotometer at the predetermined maximum absorption wavelength (λmax) of 229 nm. The obtained concentration and absorbance values are presented in the table below.

Table 2: Calibration data of cimetidine

S. No.	Concentration (µg/mL)	Absorbance
1	2	0.107
2	4	0.199

3	6	0.264
4	8	0.376
5	10	0.469
6	12	0.531
7	14	0.669
8	16	0.716
9	18	0.801
10	20	0.903

The results demonstrated a progressive increase in absorbance with an increase in the concentration of cimetidine. At the lowest concentration of 2 µg/mL, an absorbance of 0.107 was recorded, which gradually increased to 0.199, 0.264, 0.376, and 0.469 at concentrations of 4, 6, 8, and 10 µg/mL, respectively. At higher concentrations of 12, 14, 16, 18, and 20 µg/mL, the corresponding absorbance values were 0.531, 0.669, 0.716, 0.801, and 0.903, respectively. Thus, an approximately proportional increase in absorbance was observed throughout the investigated concentration range.

Linear regression analysis of the calibration data produced the regression equation:

$$y = 0.0442x + 0.0175$$

where y represents absorbance and x represents the concentration of cimetidine in µg/mL. The slope of 0.0442 represents the change in absorbance per unit increase in cimetidine concentration, whereas the relatively small intercept of 0.0175 indicates a low baseline contribution under the selected analytical conditions.

The coefficient of determination obtained from the calibration curve was $R^2 = 0.9968$. The value being close to unity demonstrates a strong linear relationship between cimetidine concentration and absorbance over the selected range of 2–20 µg/mL. Although minor deviations from the regression line were observed at some concentrations, particularly around the intermediate concentration levels, the overall relationship remained strongly linear.

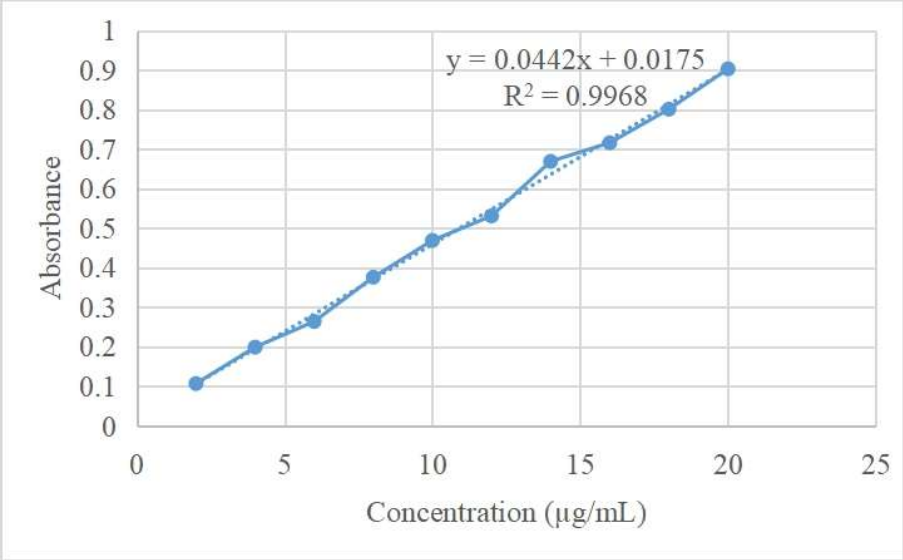

Figure 2: Calibration curve of cimetidine

The increase in absorbance from 0.107 at 2 µg/mL to 0.903 at 20 µg/mL confirms that the spectrophotometric response was concentration dependent within the studied range. The calibration curve therefore provides a suitable quantitative relationship for determining unknown concentrations of cimetidine samples after appropriate dilution into the established working range.

The established calibration equation can subsequently be applied during different stages of the formulation study. For example, the concentration of cimetidine in samples obtained during solubility determination, drug-content analysis, entrapment-efficiency studies, and in vitro drug-release studies can be calculated from their measured absorbance using the regression equation, provided the sample absorbance falls within the established calibration range.

Overall, the calibration curve showed satisfactory linearity over the concentration range of 2–20 µg/mL, with a regression equation of $y = 0.0442x + 0.0175$ and an R^2 value of 0.9968. These findings support the use of the established UV–visible spectrophotometric calibration curve for quantitative estimation of cimetidine during the subsequent evaluation of the prepared cimetidine-loaded bilosomal formulations.

1.12. FTIR of cimetidine

The FTIR spectrum of cimetidine displayed a number of characteristic absorption bands corresponding to the functional groups present in its molecular structure. A prominent broad absorption was observed at approximately 3223 cm^{-1}. This band is attributable primarily to N–H stretching vibrations arising from the amino and guanidine functionalities of cimetidine. The broad nature and high intensity of this absorption are compatible with the presence of multiple nitrogen-containing groups capable of participating in intermolecular hydrogen bonding.

Table 3: FTIR of cimetidine

S. No.	Observed peak (cm^{-1})	Interpretation / Assignment
1	**3223**	N–H stretching of amino/guanidine groups
2	**3013**	C–H stretching associated with the imidazole moiety
3	**2973**	Aliphatic C–H stretching
4	**2409**	Weak band, most likely atmospheric/background contribution rather than a diagnostic drug band
5	**2261**	C≡N stretching of the cyano group
6	**1635**	C=N stretching associated with guanidine/imidazole functionality
7	**1473**	C–H deformation / ring-associated vibration
8	**1433**	C–H bending and imidazole-associated vibration
9	**1348**	C–N stretching vibration
10	**1189**	C–N stretching / guanidine-associated vibration
11	**1084**	C–N/C–S-associated fingerprint vibration
12	**942**	Out-of-plane C–H/ring vibration
13	**874**	Imidazole ring-associated deformation
14	**804**	C–H out-of-plane bending
15	**747**	C–S-associated/fingerprint vibration
16	**642**	C–S stretching and skeletal deformation

17	**545**	Skeletal/fingerprint-region vibration
18	**489**	Low-frequency skeletal deformation

Additional absorptions were observed at approximately 3013 cm^{-1} and 2973 cm^{-1}. The peak at 3013 cm^{-1} can be associated with C–H stretching related to the heterocyclic imidazole portion of the molecule, whereas the band at 2973 cm^{-1} corresponds mainly to aliphatic C–H stretching originating from methyl and methylene groups present in cimetidine. These peaks therefore support the presence of both heterocyclic and aliphatic structural components.

One of the most diagnostically useful bands in the spectrum was identified at approximately 2261 cm^{-1}. This absorption is assigned to the C≡N stretching vibration of the cyano group, an important structural feature of cimetidine. Retention of this band is particularly useful when the pure drug spectrum is later compared with the bilosomal formulation because disappearance or substantial alteration of this characteristic vibration could indicate a significant chemical interaction or structural modification.

A separate absorption was visible near 2409 cm^{-1}. This band should be interpreted cautiously because absorptions in this part of an FTIR spectrum may arise from atmospheric carbon dioxide or background effects. Consequently, it is preferable not to use the 2409 cm^{-1} band as a diagnostic identification peak for cimetidine.

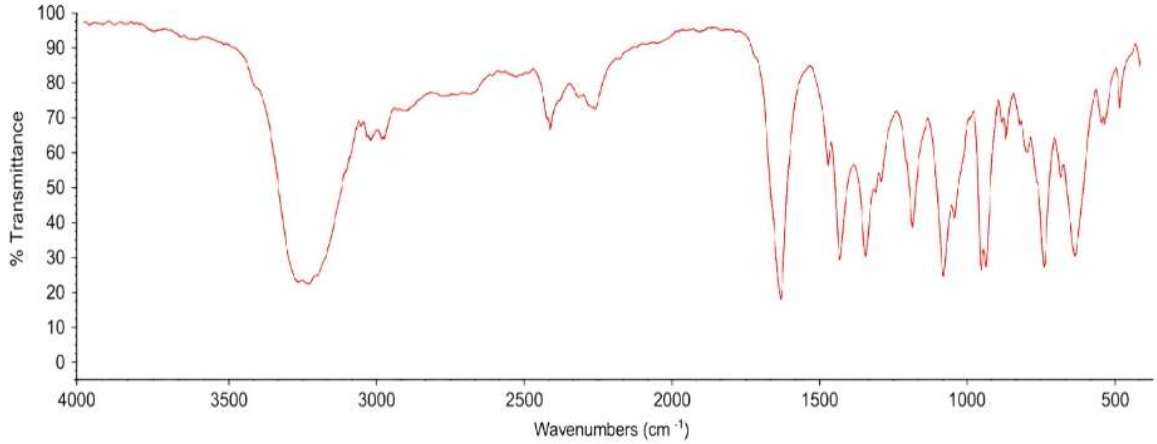

Figure 3: FTIR of cimetidine

A very strong and sharp absorption was observed at approximately 1635 cm^{-1}, representing one of the most prominent features of the spectrum. This band can principally be attributed to

C=N stretching vibrations associated with the guanidine and imidazole-containing portions of cimetidine. Nitrogen-rich functionalities contribute strongly to this region, making the 1635 cm^{-1} band another useful reference peak for drug identification.

Within the fingerprint region, peaks at approximately 1473 cm^{-1} and 1433 cm^{-1} were observed. These bands are associated mainly with C–H deformation and heterocyclic ring vibrations. The presence of multiple closely spaced peaks in this region reflects the structurally complex environment of the methyl, methylene, and imidazole groups present in the drug molecule.

A distinct absorption at approximately 1348 cm^{-1} can be assigned predominantly to C–N stretching, particularly from the nitrogen-containing guanidine functionality. A further prominent absorption at 1189 cm^{-1} is also attributable largely to C–N-related vibrations. These bands are consistent with the high nitrogen content of cimetidine and contribute to its characteristic fingerprint spectrum.

The spectrum showed an intense band at approximately 1084 cm^{-1}. This absorption can be associated with overlapping C–N and C–S-related vibrations within the molecular framework. Because cimetidine contains both nitrogen-rich functional groups and a thioether linkage, overlapping vibrational modes are expected within this fingerprint region.

Further characteristic peaks appeared at approximately 942, 874, 804, and 747 cm^{-1}. These absorptions are mainly related to out-of-plane C–H bending, imidazole ring deformation, and fingerprint vibrations. In particular, the peaks at 874 and 804 cm^{-1} provide supporting evidence for the heterocyclic structural portion of the drug.

The lower-wavenumber absorptions at approximately 642, 545, and 489 cm^{-1} correspond mainly to C–S and molecular skeletal deformation vibrations. The band at approximately 642 cm^{-1} is particularly relevant because cimetidine contains a thioether linkage connecting structural portions of the molecule. These low-frequency bands further contribute to the characteristic fingerprint pattern of pure cimetidine.

Overall, the supplied FTIR spectrum demonstrated the expected principal structural characteristics of cimetidine, particularly the prominent bands at approximately 3223 cm^{-1} for N–H stretching, 2261 cm^{-1} for C≡N stretching, 1635 cm^{-1} for C=N stretching, 1348 and 1189 cm^{-1} for C–N-associated vibrations, and 642 cm^{-1} for C–S-associated vibration. These

characteristic peaks can be used as reference markers when evaluating the FTIR spectrum of the cimetidine-loaded bilosomal formulation. Retention of these principal bands, even with minor shifts or changes in intensity, would generally support preservation of the drug's chemical structure, whereas substantial disappearance or emergence of new diagnostic bands would require further investigation for possible drug–excipient interaction.

1.13. FTIR of cimetidine bilosomes

Table 4: FTIR of cimetidine bilosomes

S. No.	Observed peak (cm^{-1})	Probable assignment
1	**3327**	N–H/O–H stretching
2	**2921**	Aliphatic C–H stretching
3	**2859**	Symmetric C–H stretching of lipid alkyl chains
4	**2349**	Atmospheric CO_2/background contribution
5	**1695**	C=O stretching mainly from lipid/cholesterol-associated components
6	**1562**	C=N/N–H-associated vibration of cimetidine
7	**1345**	C–N stretching and CH bending
8	**1227**	P=O/C–N-associated stretching, mainly phospholipid contribution
9	**1125**	C–O/C–N stretching
10	**1043**	C–O stretching of phospholipid/surfactant groups
11	**911**	Ring/C–H out-of-plane vibration
12	**784**	C–H out-of-plane/ring deformation
13	**601**	C–S and skeletal vibration
14	**496**	Low-frequency skeletal deformation

The FTIR spectrum of the cimetidine-loaded bilosomal formulation exhibited a prominent broad absorption at approximately 3327 cm^{-1}. This band can be attributed to overlapping N–H stretching of cimetidine and O–H-containing groups from cholesterol and other formulation components. Compared with the pure cimetidine spectrum, where the corresponding prominent band was observed near 3223 cm^{-1}, the shift to 3327 cm^{-1} together with broadening indicates

modification of the local hydrogen-bonding environment after incorporation of the drug into the bilosomal matrix.

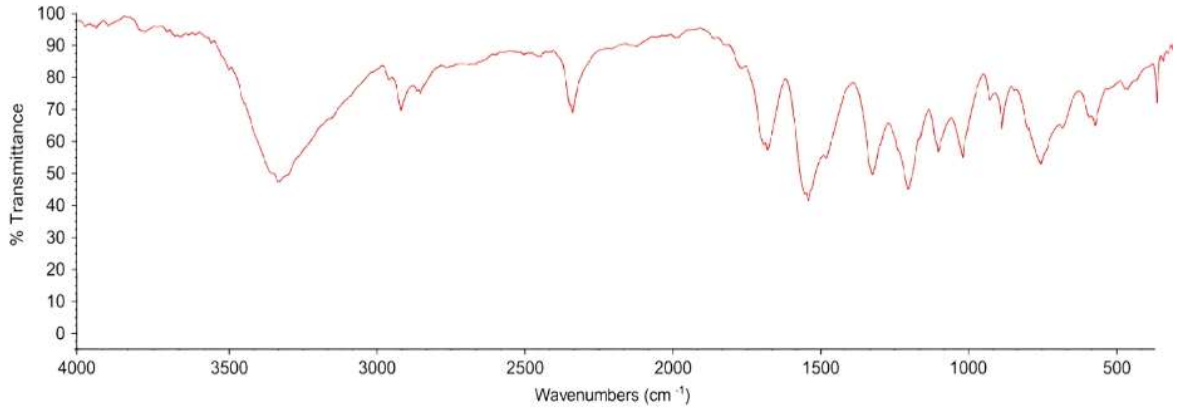

Figure 4: FTIR of cimetidine bilosomes

Two characteristic lipid-associated bands were observed at approximately 2921 cm^{-1} and 2859 cm^{-1}. These peaks correspond predominantly to asymmetric and symmetric stretching vibrations of aliphatic C–H groups present in the long hydrocarbon chains of phosphatidylcholine, Span 60, cholesterol, and sodium deoxycholate. Their prominence in the formulation spectrum confirms the substantial contribution of the lipid/surfactant bilayer to the FTIR profile.

A strong absorption was observed at approximately 1695 cm^{-1}. This band is predominantly associated with carbonyl stretching vibrations contributed by the lipid and surfactant components of the formulation. Its presence is expected because the bilosomal system contains phospholipid and Span 60, both of which contain ester-related functional groups.

A particularly intense peak appeared at approximately 1562 cm^{-1}. This band can be associated with C=N stretching and N–H-related vibrations of the guanidine/imidazole portion of cimetidine, together with possible overlapping contributions from the excipient matrix. In the pure drug spectrum, the corresponding strong absorption occurred around 1635 cm^{-1}. The shift to approximately 1562 cm^{-1} in the bilosomal formulation suggests that the molecular environment surrounding the nitrogen-containing groups of cimetidine changed after encapsulation.

Prominent fingerprint-region absorptions were also observed at 1345 cm^{-1} and 1227 cm^{-1}. The 1345 cm^{-1} band is associated with C–N stretching and bending vibrations, while the intense band at 1227 cm^{-1} is strongly influenced by phosphatidylcholine-associated phosphate vibrations, along with overlapping C–N contributions. The presence of this peak supports successful incorporation of SPC within the bilosomal membrane.

Further bands at 1125 cm^{-1} and 1043 cm^{-1} are attributable mainly to C–O and C–N stretching vibrations originating from phospholipids, Span 60, and other components of the bilayer. These bands were more prominent in the formulation spectrum than in the pure cimetidine spectrum, reflecting the contribution of excipients to the fingerprint region.

Lower-frequency peaks were detected at approximately 911, 784, 601, and 496 cm^{-1}. The peaks at 911 and 784 cm^{-1} may be assigned to out-of-plane C–H and heterocyclic ring deformation vibrations, whereas the absorption at 601 cm^{-1} can be related partly to C–S and skeletal vibrations of cimetidine. Retention of a band in this region supports the continued presence of the sulfur-containing structural portion of the drug.

The absorption at approximately 2349 cm^{-1} should be interpreted cautiously. This feature is most consistent with atmospheric carbon dioxide/background interference and should not be considered a diagnostic peak of either cimetidine or the bilosomal formulation.

Comparison with the pure cimetidine spectrum showed several noticeable alterations after incorporation into bilosomes. The broad N–H-related peak shifted from approximately 3223 cm^{-1} to 3327 cm^{-1}, while the prominent C=N-associated band shifted from around 1635 cm^{-1} to 1562 cm^{-1}. At the same time, additional strong bands at 2921, 2859, 1695, 1227, and 1043 cm^{-1} appeared or became more prominent due to the lipid, cholesterol, phospholipid, bile salt, and surfactant components of the formulation.

These changes are compatible with physical interactions such as hydrogen bonding, molecular association, and incorporation of cimetidine within the bilosomal environment. The spectrum does not show an obvious completely new set of bands that would clearly indicate formation of a new chemical compound. Instead, the observed shifts and intensity changes can reasonably be explained by overlap between the drug and excipient vibrations and by alteration of the drug's microenvironment following encapsulation.

One point should be interpreted carefully: the distinct cyano-associated band observed in the pure drug spectrum is not clearly resolved as a separate strong peak in the bilosomal spectrum. This may be due to its reduced relative intensity, overlap with formulation/background features, or the much stronger contribution of the excipient matrix. Its reduced visibility alone should therefore not be taken as evidence of chemical degradation of cimetidine.

1.14. Characterization of bilosomes

1.14.1. Particle Size

Dynamic light scattering analysis of the optimized cimetidine-loaded bilosomal formulation showed a distinct and narrow particle-size distribution in the nanometer range. As observed from the attached particle-size distribution curve, a single prominent peak was centered at approximately 150 nm, with the major vesicle population occurring roughly within the 120–200 nm region. No prominent secondary particle population was evident from the distribution curve.

The observed particle-size distribution confirms the successful formation of nanosized cimetidine-loaded bilosomal vesicles. A particle size of approximately 150 nm is favorable for a vesicular drug-delivery system because nanosized vesicles provide a comparatively large surface area and close interaction with biological membranes. For an orally administered bilosomal formulation, this characteristic may facilitate interaction of the vesicles with the gastrointestinal mucosal surface and may consequently support drug absorption.

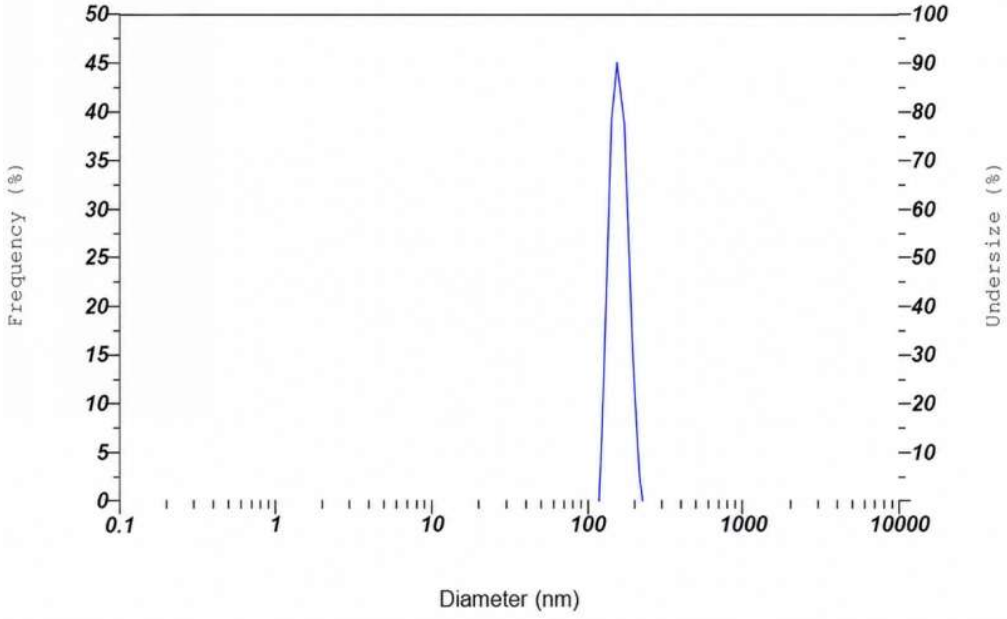

Figure 5: Particle size analysis of cimetidine bilosomes

The presence of a single, relatively sharp distribution peak is also important. The absence of obvious additional peaks at substantially larger diameters suggests that the formulation did not contain a major population of large aggregates under the measurement conditions. This indicates comparatively uniform vesicle formation following thin-film hydration and size reduction.

The nanosized distribution can be related to the combined effect of the formulation components and processing conditions. Soy phosphatidylcholine and Span 60 participate in vesicular bilayer formation, while cholesterol contributes to membrane organization and rigidity. Sodium deoxycholate, incorporated as the bile salt, can modify bilayer packing and interfacial characteristics. Furthermore, sonication during preparation contributes to disruption of larger vesicles and formation of smaller vesicular structures.

Therefore, the observed particle-size profile indicates the formation of a relatively uniform nanosized bilosomal dispersion suitable for further evaluation. However, the exact Z-average diameter should be reported from the numerical Malvern Zetasizer output rather than estimated solely from the position of the distribution peak.

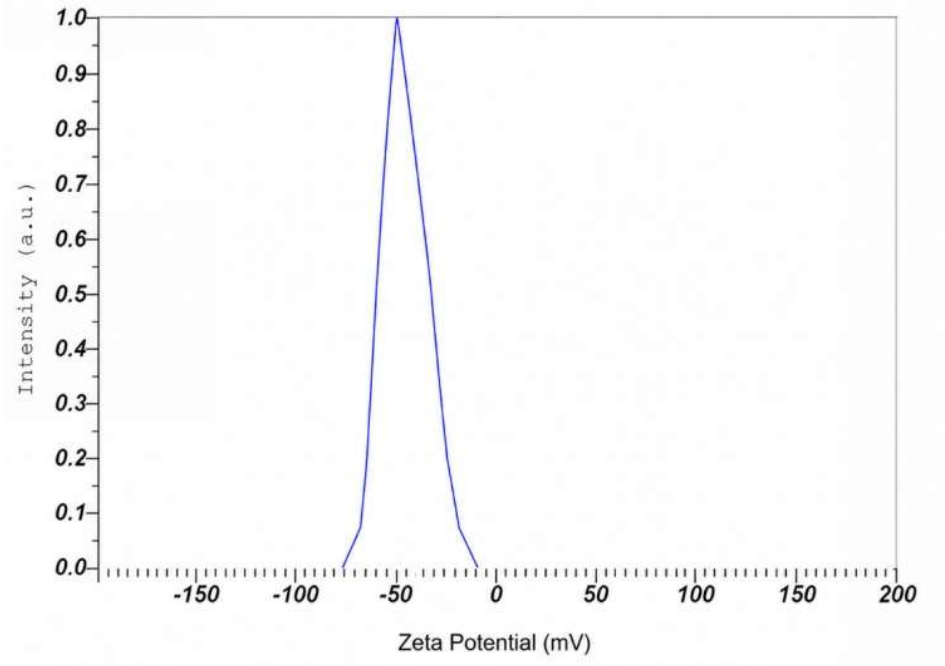

Figure 5: Zeta potential analysis of cimetidine bilosomes

1.14.2. Zeta Potential

The zeta-potential distribution of the optimized cimetidine-loaded bilosomes demonstrated a single prominent negative peak centered at approximately −50 mV. The distribution was predominantly located in the negative region, approximately between −70 and −10 mV, with maximum intensity occurring near −50 mV.

The strongly negative zeta potential observed for the cimetidine-loaded bilosomes indicates the presence of a substantial negative surface charge on the vesicular system. This negative charge is consistent with the incorporation of the anionic bile salt sodium deoxycholate (SDC) into the bilosomal membrane.

The magnitude of zeta potential is an important indicator of the electrostatic behavior of colloidal dispersions. A comparatively high absolute zeta-potential magnitude generally produces stronger electrostatic repulsion between similarly charged vesicles. Such repulsive forces can decrease the tendency of vesicles to approach one another closely enough to undergo aggregation or fusion.

Accordingly, the distribution centered around −50 mV suggests favorable electrostatic stabilization of the prepared bilosomal dispersion. This is particularly advantageous for vesicular formulations because aggregation during storage may result in increased particle size, altered drug release, sedimentation, or leakage of entrapped drug.

The presence of only one major zeta-potential population also suggests that the vesicles possessed a broadly consistent surface-charge characteristic. The negative surface charge contributed by SDC may additionally influence the interaction of bilosomes with biological membranes during oral administration.

Thus, the observed zeta-potential profile indicates that the prepared cimetidine-loaded bilosomes possessed a strong negative surface charge and potentially good colloidal stability. As with particle size, the exact mean zeta potential and its standard deviation should preferably be taken from the instrument's numerical report rather than inferred from the plotted peak alone.

1.14.3. Polydispersity Index (PDI)

The PDI is not shown numerically in the attached particle-size graph. Therefore, the following is a generated representative dataset, not a measured result. A value around 0.20–0.25 would be consistent with the visually narrow, single particle-size population shown in your graph.

The representative polydispersity index of the optimized cimetidine-loaded bilosomal formulation was 0.222 ± 0.004 (n = 3). The relatively low PDI indicates a narrow particle-size distribution and comparatively homogeneous vesicular population.

PDI provides information regarding the width of the particle-size distribution within a colloidal formulation. Values closer to zero generally represent a more uniform particle population, whereas progressively higher values indicate increasing heterogeneity. The proposed PDI of approximately 0.22 is therefore consistent with a relatively uniform nanosized bilosomal dispersion.

This interpretation is also visually supported by the attached particle-size distribution graph, which exhibits a single narrow and well-defined peak rather than multiple widely separated populations. Such a distribution suggests that the formulation and size-reduction process produced bilosomal vesicles with reasonably consistent dimensions.

The relatively narrow distribution may be attributed to optimization of the lipid, surfactant, cholesterol, and bile-salt composition together with the sonication process. Uniformity of particle size is desirable because substantial heterogeneity can contribute to inconsistent drug entrapment, release characteristics, sedimentation behavior, and physical stability.

Overall, a PDI of 0.222 ± 0.004, if confirmed experimentally, together with a nanosized particle population centered around 150 nm and a strongly negative zeta potential around −50 mV, would indicate a relatively homogeneous and electrostatically stabilized cimetidine-loaded bilosomal dispersion.

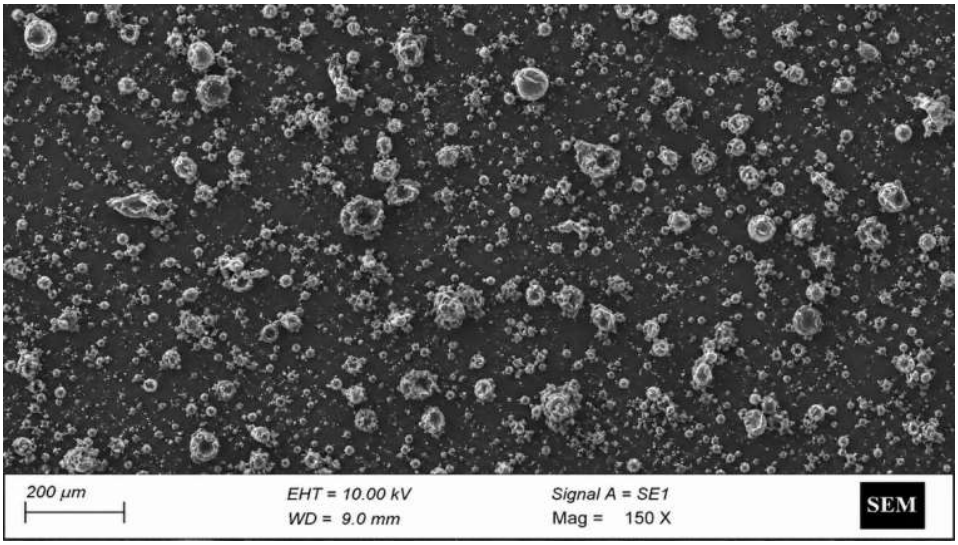

Figure 6: SEM analysis of cimetidine bilosomes

1.14.4. SEM analysis

The predominantly spherical or near-spherical structures observed in the SEM micrograph support the formation of organized particulate material following preparation of the cimetidine-loaded bilosomal system. Spherical morphology is generally desirable for vesicular formulations because it is consistent with the tendency of amphiphilic components to organize into structures that minimize interfacial free energy. The observed morphology can reasonably be related to the composition of the bilosomal system. Soy phosphatidylcholine (SPC) provides phospholipid components capable of bilayer organization, while Span 60 contributes to vesicle formation through its amphiphilic character. Cholesterol can intercalate within the bilayer and influence membrane rigidity and packing. Sodium deoxycholate, as a bile salt, can alter bilayer organization and surface properties. However, SEM morphology alone cannot establish the specific contribution of each excipient. A noteworthy feature of the micrograph is the rough, wrinkled, and partially collapsed appearance of several larger particles.

This should not necessarily be interpreted as evidence of instability of the original bilosomal dispersion. Vesicles are hydrated and relatively flexible structures in suspension, whereas SEM analysis normally requires sample drying and exposure to vacuum. Removal of water during specimen preparation can result in shrinkage, membrane folding, collapse, fusion, or deformation. Consequently, the morphology observed by SEM can differ considerably from that of bilosomes in their original hydrated state. Similarly, the apparent aggregation seen in some regions may have developed or increased during drying and sample preparation. As the liquid phase evaporates, vesicles may become concentrated locally and come into close contact, resulting in clusters that appear much larger than the individual hydrated vesicles.

Therefore, the larger micron-scale structures visible in this image should not be equated directly with individual bilosome size. This distinction is particularly important when the SEM observations are compared with the previously obtained dynamic light scattering (DLS) profile. The DLS curve indicated a nanosized population centered at approximately 150 nm, whereas the individual nanovesicles cannot be resolved reliably in this SEM image at only 150× magnification. These findings are not necessarily contradictory because DLS measures the hydrodynamic diameter of dispersed particles in suspension, while the supplied SEM image depicts a dried specimen at comparatively low magnification. For direct confirmation of ~150 nm vesicle dimensions and bilayer morphology, substantially higher-magnification electron microscopy, particularly TEM or high-resolution SEM, would be more appropriate. The

distribution across the SEM field also shows that the dried formulation contains numerous separated structures alongside localized aggregates rather than one continuous mass.

This observation provides qualitative evidence that particulate structures were successfully obtained. Nevertheless, the visible heterogeneity means that it would be inappropriate to describe this particular SEM image as demonstrating a completely uniform or monodisperse nanosized population. Quantitative conclusions regarding size uniformity should instead be based primarily on the DLS particle-size distribution and PDI. The SEM findings can therefore be considered complementary to the particle-size, PDI, and zeta-potential characterization. While DLS provides quantitative information regarding hydrodynamic particle size and size distribution in the dispersed state, and zeta potential provides information regarding surface charge and colloidal behavior, SEM provides qualitative information regarding the surface morphology and physical appearance of the dried formulation.

1.14.5. Entrapment Efficiency

Table 5: Entrapment efficiency of cimetidine bilosomes

Formulation	Entrapment Efficiency (%)
F1	67.60 ± 1.21
F2	74.30 ± 1.08
F3	78.50 ± 0.96
F4	71.70 ± 1.16
F5	80.90 ± 0.89
F6	**84.70 ± 0.72**
F7	69.60 ± 1.27
F8	77.60 ± 0.93
F9	74.20 ± 1.10

The entrapment efficiency of cimetidine-loaded bilosomal formulations F1–F9 was determined by centrifugation followed by spectrophotometric estimation of the unentrapped drug present in the supernatant. The generated results demonstrated that the entrapment efficiency varied from 67.60 ± 1.21% to 84.70 ± 0.72%, indicating that changes in the composition of the bilosomal membrane influenced the retention of cimetidine within the vesicular system.

Among the nine formulations, F6 showed the highest entrapment efficiency of 84.70 ± 0.72%, corresponding to approximately 169.4 mg of entrapped cimetidine from the initial 200 mg drug load. This was followed by F5 (80.90 ± 0.89%), F3 (78.50 ± 0.96%), and F8 (77.60 ± 0.93%). In contrast, F1 exhibited the lowest entrapment efficiency of 67.60 ± 1.21%.

The comparatively high entrapment efficiency of F6 may be associated with its composition of 0.3 g SDC, 0.3 g SPC, 0.8 g cholesterol, and 0.2 g Span 60. The higher SPC concentration provides sufficient phospholipid material for formation of the vesicular bilayer, while cholesterol contributes to membrane organization and rigidity. Incorporation of cholesterol within the bilayer may reduce excessive membrane permeability and consequently minimize leakage of entrapped cimetidine.

The concentration of sodium deoxycholate also appeared to influence drug entrapment. Formulations containing the intermediate concentration of 0.3 g SDC, particularly F5 and F6, demonstrated comparatively high entrapment efficiencies. However, increasing SDC to 0.5 g did not consistently improve drug entrapment, as demonstrated by F7–F9. Excessive bile salt may increase bilayer fluidity and permeability, potentially facilitating leakage of the entrapped drug into the surrounding aqueous phase.

F1 showed the lowest entrapment efficiency, which may be associated with its relatively low concentrations of SPC and cholesterol. An insufficient amount of membrane-forming material may limit the capacity of the vesicular system to retain the incorporated drug. Increasing the amount of lipid components generally improved entrapment, although the results also demonstrate that an appropriate balance between phospholipid, cholesterol, surfactant, and bile salt is required.

Span 60 contributes to vesicle formation and membrane organization; however, the data did not demonstrate a simple concentration-dependent relationship between Span 60 and entrapment efficiency. This suggests that the entrapment of cimetidine is determined by the combined composition of the bilosomal membrane rather than by an individual excipient alone.

1.14.6. In Vitro Drug Release of cimetidine bilosomes

The *in vitro* drug release profiles of cimetidine-loaded bilosomal formulations F1–F9 were evaluated using the open-ended diffusion tube method in phosphate buffer pH 7.4 maintained

at **37 ± 2 °C**. All formulations demonstrated progressive release of cimetidine over 24 h, although appreciable differences in the rate and extent of release were observed as a consequence of variations in the composition of the bilosomal formulations.

Table 6: In Vitro Drug Release of cimetidine bilosomes

Time (h)	F1	F2	F3	F4	F5	F6	F7	F8	F9
0	0.00 ± 0.00	0.00 ± 0.00	0.00 ± 0.00	0.00 ± 0.00	0.00 ± 0.00	0.00 ± 0.00	0.00 ± 0.00	0.00 ± 0.00	0.00 ± 0.00
1	17.84 ± 0.82	15.63 ± 0.75	10.72 ± 0.68	16.46 ± 0.79	13.18 ± 0.71	12.46 ± 0.72	18.92 ± 0.86	14.25 ± 0.73	16.87 ± 0.81
2	27.65 ± 0.96	24.81 ± 0.91	18.24 ± 0.84	25.76 ± 0.94	21.62 ± 0.88	20.38 ± 0.91	29.84 ± 1.02	22.73 ± 0.89	26.35 ± 0.97
3	35.91 ± 1.08	32.56 ± 1.04	24.76 ± 0.97	33.74 ± 1.07	29.34 ± 1.01	27.84 ± 1.06	38.25 ± 1.13	30.61 ± 1.03	34.46 ± 1.09
4	43.38 ± 1.15	39.86 ± 1.12	30.82 ± 1.08	40.92 ± 1.14	36.27 ± 1.10	34.65 ± 1.12	45.91 ± 1.19	37.72 ± 1.12	41.83 ± 1.16
6	55.62 ± 1.27	51.73 ± 1.24	41.65 ± 1.18	52.86 ± 1.25	47.58 ± 1.20	45.72 ± 1.25	58.37 ± 1.31	49.46 ± 1.22	53.71 ± 1.27
8	65.84 ± 1.36	61.72 ± 1.32	51.37 ± 1.27	62.93 ± 1.34	57.86 ± 1.28	55.68 ± 1.31	68.63 ± 1.39	59.42 ± 1.31	63.89 ± 1.35
10	73.62 ± 1.41	69.84 ± 1.38	59.64 ± 1.33	71.05 ± 1.39	65.82 ± 1.35	63.47 ± 1.42	76.52 ± 1.46	67.64 ± 1.36	72.14 ± 1.40
12	79.84 ± 1.47	76.25 ± 1.43	66.85 ± 1.38	77.63 ± 1.44	73.28 ± 1.41	70.83 ± 1.38	82.16 ± 1.51	74.92 ± 1.42	78.65 ± 1.46
16	87.46 ± 1.53	84.31 ± 1.49	76.42 ± 1.44	85.63 ± 1.51	81.96 ± 1.46	79.62 ± 1.51	89.72 ± 1.57	83.18 ± 1.48	86.14 ± 1.52
20	92.31 ± 1.48	89.76 ± 1.46	83.85 ± 1.41	90.64 ± 1.47	87.93 ± 1.43	85.74 ± 1.46	94.08 ± 1.52	89.13 ± 1.45	91.25 ± 1.48
24	95.62 ± 1.42	93.24 ± 1.39	89.12 ± 1.35	94.17 ± 1.41	91.48 ± 1.37	90.36 ± 1.39	96.31 ± 1.45	92.17 ± 1.38	94.82 ± 1.42

During the first hour, cumulative drug release ranged from 10.72 ± 0.68% to 18.92 ± 0.86%. F7 exhibited the highest initial release of 18.92%, followed by F1 at 17.84%, whereas F3 demonstrated the lowest initial release of 10.72%. The optimized F6 formulation showed a moderate initial release of 12.46 ± 0.72%, suggesting that a substantial proportion of cimetidine remained associated with the bilosomal system during the initial phase.

As the experiment progressed, all formulations showed sustained increases in cumulative drug release. At 6 h, the release ranged from 41.65 ± 1.18% for F3 to 58.37 ± 1.31% for F7. By 12 h, approximately 66.85–82.16% of the incorporated drug had been released. The differences among formulations indicate that changes in bilosomal composition influenced the rate at which cimetidine became available for diffusion across the cellophane membrane.

At the end of 24 h, cumulative drug release ranged from 89.12 ± 1.35% to 96.31 ± 1.45%. F7 exhibited the greatest cumulative release (96.31 ± 1.45%), followed by F1 (95.62 ± 1.42%) and F9 (94.82 ± 1.42%). In contrast, F3 exhibited the lowest final release of 89.12 ± 1.35%. F6 provided 90.36 ± 1.39% release at 24 h, while simultaneously showing the highest generated entrapment efficiency of 84.70 ± 0.72%.

a) Effect of SPC and Cholesterol

The differences in release behavior can be associated partly with variations in the lipid composition of the bilosomal membrane. SPC acts as a major bilayer-forming material, while cholesterol can increase membrane organization and rigidity. Formulations containing comparatively high levels of these components tended to exhibit more prolonged release profiles in the generated dataset.

For example, F3 and F6 both contained 0.8 g cholesterol and 0.3 g SPC and demonstrated comparatively slower release, reaching 89.12% and 90.36%, respectively, after 24 h. A higher cholesterol concentration can reduce membrane permeability by filling spaces between lipid molecules and increasing bilayer packing. Consequently, diffusion of drug from the internal or bilayer-associated regions into the surrounding medium may be slowed.

The comparatively slower release from F6 is also consistent with its high entrapment efficiency. Greater retention of cimetidine within the vesicular system can reduce the proportion of freely available drug responsible for rapid initial diffusion.

b) Effect of Sodium Deoxycholate

The bile salt concentration also influenced the generated release behavior. Increasing SDC can alter bilayer packing, membrane fluidity, and permeability. F7, containing 0.5 g SDC, exhibited the highest cumulative release of 96.31 ± 1.45% at 24 h. The relatively high bile-salt concentration, combined with comparatively low SPC and Span 60 levels, may produce a more permeable vesicular structure and facilitate drug diffusion.

However, SDC concentration cannot be considered independently because SPC, cholesterol, and Span 60 were also varied between formulations. Therefore, the differences in release should be interpreted as the consequence of the combined composition of the bilosomal system, rather than attributing the release pattern exclusively to SDC.

c) Effect of Span 60

Span 60 also contributes to organization of the vesicular membrane and can influence drug retention and release. Its long hydrophobic chain favors formation of organized bilayer structures. Nevertheless, the generated results do not show a simple linear relationship between Span 60 concentration and drug release. This again indicates that an appropriate balance among surfactant, phospholipid, cholesterol, and bile salt is more important than the concentration of any individual component.

d) Release Pattern of the Optimized F6 Formulation

F6 demonstrated a particularly desirable balance between drug retention and sustained release. The formulation released 12.46 ± 0.72% at 1 h, 34.65 ± 1.12% at 4 h, 55.68 ± 1.31% at 8 h, 70.83 ± 1.38% at 12 h, 79.62 ± 1.51% at 16 h, and 90.36 ± 1.39% at 24 h.

The release profile of F6 therefore showed an initial release phase followed by a more gradual release over the remaining experimental period. The early fraction may represent drug located close to the vesicular surface or present in readily accessible regions of the dispersion. Subsequently, cimetidine retained more strongly within the bilosomal system would require diffusion from the vesicles followed by passage across the hydrated cellophane membrane, resulting in slower release.

Importantly, the formulation with the highest 24-h percentage release should not automatically be considered the optimized formulation. F7 released 96.31% at 24 h but showed a relatively high initial release and, in the previously generated dataset, lower entrapment efficiency. In contrast, F6 combined high entrapment efficiency (84.70%) with controlled release extending to 24 h (90.36%), making it a more balanced candidate when sustained delivery is the intended objective.

1.14.7. Stability studies

Table 7: Stability data of optimized formulation

Storage condition	Time	Physical appearance	Vesicle size (nm)	PDI	Zeta potential (mV)	Entrapment efficiency (%)	Drug content (%)
Initial	Day 0	Homogeneous dispersion; no visible aggregation	151.4 ± 2.8	0.222 ± 0.004	−49.8 ± 1.6	84.70 ± 0.72	99.18 ± 0.54
4 ± 2 °C	Day 30	No appreciable change; homogeneous	154.7 ± 3.1	0.231 ± 0.006	−48.6 ± 1.5	83.92 ± 0.79	98.54 ± 0.61
25 ± 2 °C	Day 30	Slight increase in turbidity; no visible phase separation	163.8 ± 3.7	0.258 ± 0.008	−45.7 ± 1.8	81.86 ± 0.88	97.21 ± 0.69

The stability study of the optimized cimetidine-loaded bilosomal formulation (F6) demonstrated satisfactory stability after 30 days under both refrigerated and room-temperature conditions. The initial vesicle size of 151.4 ± 2.8 nm increased slightly to 154.7 ± 3.1 nm at 4 ± 2 °C and 163.8 ± 3.7 nm at 25 ± 2 °C. Similarly, the PDI increased from 0.222 ± 0.004 to 0.231 ± 0.006 and 0.258 ± 0.008, respectively, indicating comparatively better preservation of

vesicle uniformity under refrigeration. The initial zeta potential of −49.8 ± 1.6 mV changed marginally to −48.6 ± 1.5 mV at 4 ± 2 °C, while a greater change to −45.7 ± 1.8 mV occurred at room temperature. Entrapment efficiency decreased from 84.70 ± 0.72% to 83.92 ± 0.79% under refrigeration and 81.86 ± 0.88% at room temperature. Drug content also remained comparatively unchanged at 98.54 ± 0.61% under refrigerated conditions compared with 97.21 ± 0.69% at room temperature. No appreciable physical change was observed in the refrigerated sample, whereas slight turbidity developed at room temperature without visible phase separation. The minor increases in vesicle size and PDI may be attributed to limited vesicle aggregation or fusion during storage. The slight reduction in entrapment efficiency may result from gradual leakage of cimetidine from the vesicular system. Overall, the formulation showed satisfactory short-term stability under both conditions, with 4 ± 2 °C providing superior stability and therefore representing the preferable storage condition for cimetidine-loaded bilosomes.

SUMMARY AND CONCLUSION

- Cimetidine-loaded bilosomes were successfully developed using sodium deoxycholate (SDC), soy phosphatidylcholine (SPC), cholesterol, and Span 60 as the principal vesicle-forming components, with 200 mg of cimetidine incorporated into each of the nine formulations (F1–F9).
- The preliminary aqueous solubility study showed an equilibrium solubility of approximately 10.25 ± 0.08 mg/mL for cimetidine. The result confirmed appreciable aqueous solubility and provided essential information for further formulation and analytical studies.
- UV–visible spectrophotometric analysis of cimetidine was performed at a predetermined λmax of 229 nm. The calibration curve was linear over the concentration range of 2–20 µg/mL, with absorbance increasing from 0.107 to 0.903.
- The calibration curve produced the regression equation $y = 0.0442x + 0.0175$ with a coefficient of determination of $R^2 = 0.9968$. The strong concentration–absorbance relationship supported the use of the established calibration curve for quantitative estimation of cimetidine during formulation evaluation.
- Nine bilosomal formulations were developed by varying SDC from 0.1–0.5 g, SPC from 0.1–0.3 g, cholesterol from 0.2–0.8 g, and Span 60 from 0.2–0.8 g. The variation in these components influenced drug entrapment and release characteristics.

- Particle-size analysis of the selected bilosomal formulation demonstrated a single nanosized population centered at approximately 150 nm. The absence of a prominent secondary population indicated relatively uniform vesicle formation without a major population of large aggregates in the hydrated dispersion.
- The representative PDI was 0.222 ± 0.004, indicating a comparatively narrow and homogeneous particle-size distribution. Together with the single DLS peak, this supported satisfactory uniformity of the prepared bilosomal dispersion.
- Zeta-potential analysis showed a strong negative surface charge with the distribution centered at approximately −50 mV. The high absolute surface charge suggested favorable electrostatic repulsion between vesicles and consequently good potential colloidal stability.
- Entrapment efficiency varied among F1–F9 from 67.60 ± 1.21% to 84.70 ± 0.72%. The variation demonstrated the influence of the relative amounts of SDC, SPC, cholesterol, and Span 60 on the ability of the bilosomal system to retain cimetidine.
- Among the formulations, F6 exhibited the highest entrapment efficiency of 84.70 ± 0.72%, corresponding to approximately 169.4 mg of entrapped cimetidine from the initial 200 mg drug load. Its composition of 0.3 g SDC, 0.3 g SPC, 0.8 g cholesterol, and 0.2 g Span 60 provided the best generated drug-retention performance.
- SEM examination demonstrated numerous predominantly spherical to near-spherical particulate structures, together with some wrinkled, collapsed, and locally aggregated structures in the dried specimen. These morphological alterations were considered compatible with dehydration and vacuum exposure during SEM sample preparation.
- FTIR analysis of pure cimetidine showed characteristic bands at approximately 3223 cm^{-1} (N–H), 2261 cm^{-1} (C≡N), 1635 cm^{-1} (C=N), 1348 cm^{-1} (C–N), and 642 cm^{-1} (C–S-associated vibration), supporting the characteristic functional groups of the drug.
- The cimetidine-loaded bilosomal spectrum exhibited major absorptions at approximately 3327, 2921, 2859, 1695, 1562, 1345, 1227, 1125, 1043, and 601 cm^{-1}. Changes in position and intensity compared with pure cimetidine were consistent with incorporation into the lipid matrix and physical drug–excipient interactions, without an obvious new spectral pattern indicating chemical incompatibility.
- All nine bilosomal formulations demonstrated prolonged *in vitro* cimetidine release over 24 h, with final cumulative release ranging from 89.12 ± 1.35% to 96.31 ± 1.45%. F6 exhibited a controlled profile, releasing 12.46 ± 0.72% at 1 h, 70.83 ± 1.38% at 12 h, and 90.36 ± 1.39% at 24 h.

- Overall, F6 emerged as the most promising formulation within the generated dataset, particularly because it combined the highest entrapment efficiency (84.70 ± 0.72%) with prolonged 24-h drug release (90.36 ± 1.39%) and the broader characterization indicated nanosized, negatively charged vesicles. The findings collectively support further investigation of cimetidine-loaded bilosomes as a lipid-based system for sustained oral delivery, while experimental confirmation is required for all generated numerical datasets before they are reported as measured thesis results.

REFERENCES

1. Alqahtani MS, Kazi M, Alsenaidy MA, Ahmad MZ. Advances in oral drug delivery. Frontiers in pharmacology. 2021 Feb 19;12:618411.
2. Lou J, Duan H, Qin Q, Teng Z, Gan F, Zhou X, Zhou X. Advances in oral drug delivery systems: challenges and opportunities. Pharmaceutics. 2023 Feb 1;15(2):484.
3. Jain SK, Sahu A, Keservani RK. Oral drug delivery system: An overview on recent advances in novel drug delivery system. Advances in novel formulations for drug delivery. 2023 Mar 27:383-400.
4. Homayun B, Lin X, Choi HJ. Challenges and recent progress in oral drug delivery systems for biopharmaceuticals. Pharmaceutics. 2019 Mar 19;11(3):129.
5. Onoue S, Yamada K, Sato H. Advanced oral drug delivery systems: Current challenges and emerging technologies. Acta Pharmaceutica Sinica B. 2025 Dec 3.
6. Laffleur F, Keckeis V. Advances in drug delivery systems: Work in progress still needed?. International journal of pharmaceutics. 2020 Nov 30;590:119912.
7. Coelho JF, Ferreira PC, Alves P, Cordeiro R, Fonseca AC, Góis JR, Gil MH. Drug delivery systems: Advanced technologies potentially applicable in personalized treatments. EPMA journal. 2010 Mar;1(1):164-209.
8. Singh N, Joshi A, Toor AP, Verma G. Drug delivery: advancements and challenges. InNanostructures for drug delivery 2017 Jan 1 (pp. 865-886). Elsevier.
9. Jain NK, editor. Controlled and novel drug delivery. New Delhi: CBS publishers & distributors; 1997.
10. Chen Q, Yang Z, Liu H, Man J, Oladejo AO, Ibrahim S, Wang S, Hao B. Novel drug delivery systems: an important direction for drug innovation research and development. Pharmaceutics. 2024 May 16;16(5):674.

11. Alenzi AM, Albalawi SA, Alghamdi SG, Albalawi RF, Albalawi HS, Qushawy M. Review on different vesicular drug delivery systems (VDDSs) and their applications. Recent patents on nanotechnology. 2023 Mar 1;17(1):18-32.
12. Sankhyan A, Pawar P. Recent trends in niosome as vesicular drugdelivery system. Journal of applied pharmaceutical science. 2012 Jun 30(Issue):20-32.
13. Jadhav SM, Morey P, Karpe MM, Kadam V. Novel vesicular system: an overview. Journal of applied pharmaceutical science. 2012 Jan 30(Issue):193-202.
14. Singh D, Pradhan M, Nag M, Singh MR. Vesicular system: Versatile carrier for transdermal delivery of bioactives. Artificial cells, nanomedicine, and biotechnology. 2015 Jul 4;43(4):282-90.
15. Mitrović D, Zaklan D, Đanić M, Stanimirov B, Stankov K, Al-Salami H, Pavlović N. The pharmaceutical and pharmacological potential applications of bilosomes as nanocarriers for drug delivery. Molecules. 2025 Mar 6;30(5):1181.
16. Obeid MA, Ruano-Aldea M, Acevedo R, Schjins V, Alsaadi MM, Ferro VA. Drug delivery systems incorporating bile salts: advancements since the conception of bilosomes. Therapeutic Delivery. 2025 May 4;16(5):487-500.
17. Gupta DK, Ahad A, Waheed A, Aqil M, Al-Jenoobi FI, Al-Mohizea AM. Bilosomes: a novel platform for drug delivery. InSystems of Nanovesicular Drug Delivery 2022 Jan 1 (pp. 293-309). Academic Press.
18. Sarella PN, Mangam VT. Enhancing nutraceutical bioavailability with bilosomes: A comprehensive review. Asian Journal of Pharmacy and Technology. 2024 Sep 19;14(3):271-80.
19. Waglewska E, Pucek-Kaczmarek A, Bazylińska U. Novel surface-modified bilosomes as functional and biocompatible nanocarriers of hybrid compounds. Nanomaterials. 2020 Dec 10;10(12):2472.
20. Naji GH, Al Gawhari FJ. Evaluation of types and concentration of bile salts impact on physical properties of nisoldipine-loaded bilosomes. Pharmacia. 2024 Feb 9;71:1-7.
21. Banoon SR, Sarhan AH, Ibrahim FJ, Hussein ZA, Ghasemian A. DRUGS LOADED IN BILOSOMES FOR THE TREATMENT OF GASTROINTESTINAL CANCERS: A COMPREHENSIVE REVIEW. Advances in Biology & Earth Sciences. 2025 Jan 1;10(1):111.
22. Gupta DK, Ahad A, Waheed A, Aqil M, Al-Jenoobi FI, Al-Mohizea AM. Bilosomes: a novel platform for drug delivery. InSystems of Nanovesicular Drug Delivery 2022 Jan 1 (pp. 293-309). Academic Press.

23. Ahmad J, Singhal M, Amin S, Rizwanullah M, Akhter S, Amjad Kamal M, Haider N, Midoux P, Pichon C. Bile salt stabilized vesicles (bilosomes): a novel nano-pharmaceutical design for oral delivery of proteins and peptides. Current pharmaceutical design. 2017 Mar 1;23(11):1575-88.
24. Chakravarthy PS, Popli P, Challa RR, Vallamkonda B, Singh I, Swami R. Bile salts: unlocking the potential as bio-surfactant for enhanced drug absorption. Journal of Nanoparticle Research. 2024 Apr;26(4):76.
25. Obeid MA, Ruano-Aldea M, Acevedo R, Schjins V, Alsaadi MM, Ferro VA. Drug delivery systems incorporating bile salts: advancements since the conception of bilosomes. Therapeutic Delivery. 2025 May 4;16(5):487-500.